# Characterization of $Cr^{3+}$ centres in $LiNbO_3$ using fluorescence line narrowing



1995 J. Phys.: Condens. Matter 7 9643

(http://iopscience.iop.org/0953-8984/7/49/026)

J. Phys.: Condens. Matter 7 (1995) 9643–9656. Printed in the UK

# Characterization of $Cr^{3+}$ centres in $LiNbO_3$ using fluorescence line narrowing

Peter I Macfarlane, Keith Holliday, John F H Nicholls and Brian Henderson
Department of Physics and Applied Physics, University of Strathclyde, Glasgow G1 1XN, UK

Received 29 August 1995

**Abstract.** The optical spectroscopic properties of $Cr^{3+}$ in $LiNbO_3$ have been investigated using optical absorption, fluorescence, fluorescence line narrowing (FLN), selective excitation and radiative lifetime measurements. The present results are compared with data obtained using other techniques including electron spin resonance (ESR) and electron nuclear double resonance (ENDOR), and shown to be consistent with there being five $Cr^{3+}$ centres. The predominant centre is due to substitution at the $Li^+$ site, which provides the weak crystal field in which $Cr^{3+}$ ions emit into a broad $^4T_2 \rightarrow {}^4A_2$ band. Using FLN, two centres experiencing a stronger crystal field are shown to be due to substitution at this same site, probably perturbed by the location of $Nb^{5+}$ antisites and $Nb^{5+}$ vacancies in the next-nearest-neighbour cation shell.

The addition of $Mg^{2+}$ ions to $LiNbO_3$ appears not to create new $Cr^{3+}$ complexes: rather it modifies the nature of the disorder, thereby changing the relative concentrations of the different centres. To this extent it becomes possible to identify two other lightly occupied $Cr^{3+}$ centres where substitution is at the $Nb^{5+}$ site. This total of five $Cr^{3+}$ centres in $LiNbO_3$ gives a consistent interpretation of all the available spectroscopic evidence, including ESR and ENDOR, while pointing to the difficulties of theoretical work in sites where the differences in the energy levels of $Cr^{3+}$ ions are too small to be distinguished by the available models.

## 1. Introduction

$Cr^{3+}$ ions in lithium niobate ($LiNbO_3$) emit broad band luminescence when excited with visible light, and this observation has stimulated many recent spectroscopic studies of $Cr^{3+}$:$LiNbO_3$. These investigations have revealed that the material also fluoresces via a number of much narrower R lines. The results of such studies are not fully understood and different researchers have drawn conflicting conclusions.

It is well known that in strong-field sites at low temperature the luminescence of $Cr^{3+}$ ions is predominantly via the $^2E \rightarrow {}^4A_2$ transition (R lines), whereas in weak-field sites the broad-band $^4T_1 \rightarrow {}^4A_2$ transition is dominant. It should be noted that the difference in crystal-field strength between weak- and strong-field sites may actually be very small; the distinction is between sets of ions experiencing an intermediate crystal field close to the crossing between $^4T_2$ and $^2E$ states. For the purposes of this paper, a strong crystal field is defined as resulting in the $^2E$ state being lower than the $^4T_2$ state and vice versa for weak crystal fields. The simultaneous presence of several R lines and broad-band fluorescence suggests that $Cr^{3+}$ ions substitute into multiple environments in $LiNbO_3$.

The structure of $LiNbO_3$ below its ferroelectric Curie temperature belongs to the $R3c$ space group [1]. Shown schematically in figure 1 are the three interlocking octahedral complexes that repeat to compose the crystal structure. These three complexes are each defined by the central ion (or void) and are stacked along the $c$ axis in the sequence

0953-8984/95/499643+14$19.50  

Li, Nb, empty octahedron, Li, Nb, empty octahedron, etc, each separated by planes of oxygen ions. The symmetry at the $Li^+$ and $Nb^{5+}$ sites and the empty octahedron is $C_3$, although $C_{3v}$ is often regarded as a good approximation [2, 3]. All three sites are candidates for occupancy by the dopant $Cr^{3+}$ ion given the preference this ion has for octahedral coordination. Although stoichiometric crystals are grown, it is easier to grow $LiNbO_3$ crystals with the congruent composition, $(Li_{1-5x}Nb_{5x})Nb_{1-4x}O_3$, where $x \approx 0.0118$. This formula implies that almost 6% of $Li^+$ sites are occupied by $Nb^{5+}$ ions (referred to as Nb antisites) and that an appropriate number of $Nb^{5+}$ sites are vacant to ensure charge neutrality [1, 4].

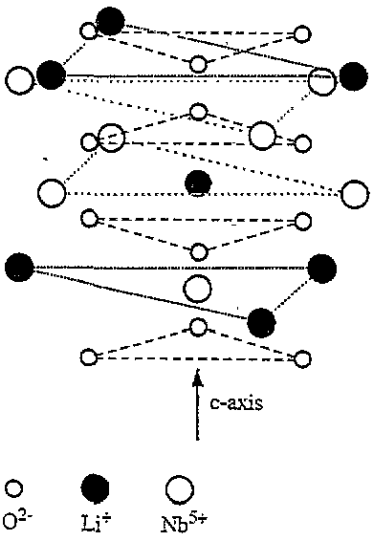


**Figure 1.** A schematic representation of the structure of $LiNbO_3$. The central $Li^+$ site is surrounded by an approximate octahedron of nearest-neighbour $O^{2-}$ ions, an approximate octahedron of second-nearest-neighbour $Nb^{5+}$ ions and a slightly larger approximate octahedron of $Li^+$ ions. Interlocking octahedra of oxygen ions are defined by the occupation of their central position and follow along the *c* axis in the order empty octahedron, $Li^+$, $Nb^{5+}$. The guide lines on the figure indicate triangles of like ions in the *ab* plane.

In order to make $LiNbO_3$ more resistant to damage in frequency doubling applications it is common practice to add MgO to the melt, thus causing an additional source of disorder within the lattice. The non-stoichiometry of the crystals, the influence of $Mg^{2+}$ codoping and the many possibilities for charge compensation that result from $Cr^{3+}$ ions substituting into a lattice with no triply ionized host ions lead to complicated optical and magnetic spin resonance spectra for $Cr^{3+}$:$LiNbO_3$ and $Cr^{3+}$:$Mg^{2+}$:$LiNbO_3$. First reports of these spectra appeared in 1966 [5] and have remained the subject of much debate.

The objective of the present study is to resolve the contradictory conclusions that have been drawn by various workers. High-resolution laser spectroscopic measurements of $Cr^{3+}$:$LiNbO_3$ and $Cr^{3+}$:$Mg^{2+}$:$LiNbO_3$ have been conducted to make possible a definitive interpretation of the optical spectra. These results have also been used to interpret the observed optical spectra in a manner consistent with all the published ESR and ENDOR results. This has made it possible to develop a realistic model of the site occupancy of $Cr^{3+}$ ions in $LiNbO_3$ and MgO–$LiNbO_3$.

## 2. Experimental methods

Optical absorption spectra were measured using an AVIV spectrophotometer that operated in the wavelength range 190–3000 nm. The samples were cooled to 77 K in a liquid nitrogen cryostat. In photoluminescence experiments the samples were cooled to 15 K in a cryorefrigerator. The broad-band luminescence was excited by a dye laser, the emitted radiation being dispersed in a 0.5 m monochromator and detected by a germanium detector. Corrections were made for the spectral response of the system.

In FLN studies the R lines were excited by the highly monochromatic output from a tuneable Ti:sapphire laser, which has a jitter-limited linewidth of less than 1 MHz. The luminescence was dispersed in a 1 m monochromator and detected using photon counting electronics. In order to measure the splitting of the $^4A_2$ ground state, higher-resolution spectra were obtained by analysing the radiation emitted by the sample with a scanning Fabry–Perot etalon, placed before the 1 m grating monochromator to isolate the specific spectral range of interest. The etalon plates were set 1 mm apart giving a free spectral range of 5 $cm^{-1}$ with a transmission linewidth of 0.1 $cm^{-1}$. In these FLN studies the wavelength of excitation was measured using a wavemeter. The R line luminescence in $LiNbO_3$ is very weak; the short lifetime and the necessity to use a monochromator for auxiliary dispersion meant that time-resolved spectra composed of resonant and non-resonant lines could not be obtained. The ground state splittings of the R lines were therefore determined using cw excitation, the strong laser scatter in the resulting spectrum marking the resonant condition whilst much weaker non-resonant features correspond to fluorescence from the sample decaying to the alternative ground state level.

## 3. Results and discussion

### *3.1. General spectroscopic measurements*

The optical spectroscopy of $Cr^{3+}$ ions in $LiNbO_3$ was reported first by Burns *et al* [5]. They identified two sharp R lines in absorption at wavelengths of 724.2 nm and 726.2 nm due to $^4A_2 \rightarrow {}^2E$ transitions split by a trigonal field. They also observed the broad $^4A_2 \rightarrow {}^4T_2$, $^4T_1$ absorption bands spanning the visible region. The $Cr^{3+}$:$LiNbO_3$ sample used in this study gave similar absorption spectra (figure 2). Also shown in figure 2, superposed on the broad absorption bands, are sharper features associated with spin-forbidden transitions from the $^4A_2$ ground state to the $^2T_1$ and $^2T_2$ levels.

To check the validity of the transition assignments, crystal-field theory is applied to calculate the energies of the states. Sugano and coworkers [6] derived the energy matrices for the term splittings of 3d electrons in octahedral fields and these have been applied successfully to interpret the observed optical spectra of transition metal ions in many host crystals. The matrices depend on the strength of the octahedral crystal field, Dq, and the Racah parameters $B$ and $C$. The peak energy of the $^4A_2 \rightarrow {}^4T_2$ band is 10 Dq, after defining the ground state $^4A_2$ to be the energy zero. Diagonalizing the $2 \times 2$ matrix of the $^4T_1$ terms to fit the peak of the $^4A_2 \rightarrow {}^4T_1$ band yields the $B$ parameter, and the $C$ parameter is obtained from the energy of the $^2E$ level. The energies of the other levels are then calculated by diagonalizing the appropriate matrices. The calculated and observed energies given in table 1 are in good agreement, although the results of these calculations are valid only for the dominant centre that is introduced below as the $\gamma$ centre.

The broad luminescence band, excited in either the $^4A_2 \rightarrow {}^4T_2$ band and peaking at 900 nm, was also first observed by Burns *et al* [5], and was tentatively identified with the

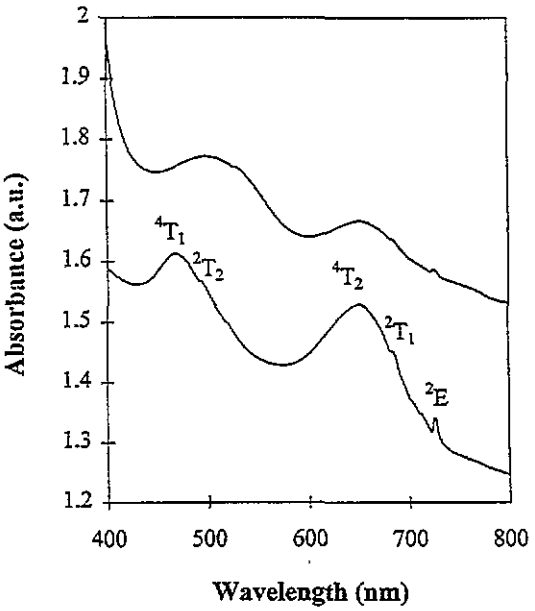


*Figure 2. Optical absorption spectra of $Cr^{3+}$ ions in $LiNbO_3$ (lower) and $MgO:LiNbO_3$ (upper) measured at room temperature.*

**Table 1.** Calculated energies of multiplets of $Cr^{3+}$ in $LiNbO_3$ using the octahedral approximation. $Dq = 1530\ cm^{-1}$, $C = 3204\ cm^{-1}$ and $B = 558\ cm^{-1}$.

| Level | Calculated energy ($cm^{-1}$) | Observed energy ($cm^{-1}$) |
|---|---|---|
| $^2E$ | 13 798 | 13 790 |
| $^2T_1$ | 14 254 | 14 340 |
| $^4T_2$ | 15 300 | 15 300 |
| $^2T_2$ | 20 640 | 20 200 |
| $^4T_1$ | 21 000 | 21 000 |

Stokes-shifted $^4T_2 \rightarrow {}^4A_2$ transition. In the present study it was found that the broad emission lineshape (figure 3(a)) is independent of excitation wavelength except at the low-energy wing of the $^4A_2 \rightarrow {}^4T_2$ absorption band near 750 nm, where the resulting emission is red shifted by around 50 nm.

The fluorescence spectrum contains three sharp lines near 730 nm (figure 3(b)), two of which were first reported by Glass [7]. The integrated intensity of these lines is of the order of one-thousandth of that of the broad band. These lines have been identified with the $^2E \rightarrow {}^4A_2$ transitions, resulting from two overlapping R line pairs due to $^2E$ states split by the combined effects of trigonal field and spin–orbit coupling [8, 9]. The line at 735.5 nm is an $R_1$ line whose $R_2$ partner at 730.4 nm is degenerate with an $R_1$ line having its partner at 727.0 nm. The wavelengths of these R lines are quite different from those measured in absorption. These results lead to the important conclusion that in $LiNbO_3$ there are three distinct $Cr^{3+}$ environments, producing three distinct R line systems. For purposes of identification the lowest-energy doublet, at 735.5 nm and 730.4 nm, is designated the $R_{1,2}(\alpha)$ lines, the lines at 730.4 nm and 727.0 nm are the $R_{1,2}(\beta)$ lines and the R lines observed in absorption (726.2 nm and 724.2 nm) are termed $R_{1,2}(\gamma)$. The corresponding

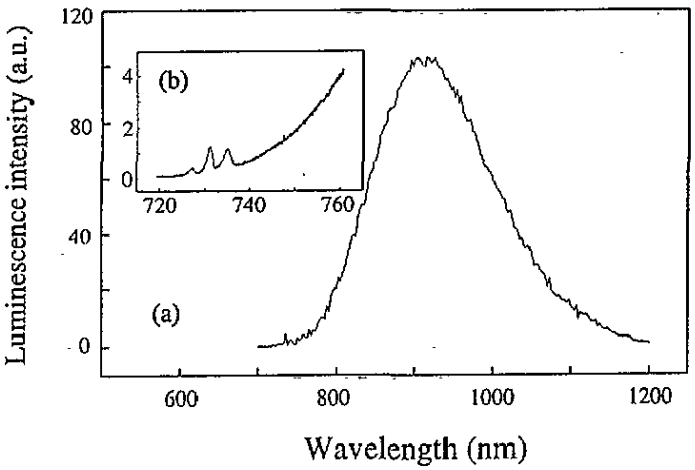


**Figure 3.** (a) The broad-band luminescence and (b) the R lines in emission from $Cr^{3+}$ : $LiNbO_3$ measured at 15 K.

centres are referred to as $\alpha$, $\beta$ and $\gamma$, respectively. The $\gamma$ centre emits from the $^2E$ level as $R_{1,2}(\gamma)$ lines at elevated temperatures through thermal depopulation of the $^4T_2$ level. Weiyi *et al* [8] attributed this emission to hot-phonon sidebands of the $^4T_2$ zero-phonon lines. However, in view of the similarity in energy, linewidths and splittings of these lines to the other R lines this explanation is unlikely. Evidence from excitation spectra completely rule out this interpretation.

Scanning the Ti:sapphire laser over the R line region in the absorption spectrum and detecting luminescence at 850 nm strongly picks out the $R_{1,2}(\gamma)$ lines, confirming the excitation spectrum published previously [8]. This demonstrates emphatically that the $R_{1,2}(\gamma)$ absorption lines and the 900 nm photoluminescence band originate from $Cr^{3+}$ ions at the same weak-field site. Indeed, the entire optical spectrum of $Cr^{3+}$:$LiNbO_3$ is dominated by features associated with the $\gamma$ centre, the R lines from centres $\alpha$ and $\beta$ being almost undetectable in absorption and dwarfed by the broad band in luminescence (figure 3). In consequence it follows that the $^4A_2 \rightarrow {}^4T_2$, $^4T_1$ absorption peaks in figure 2 also originate predominantly from the weak-field centre, $\gamma$.

The $^2E \leftrightarrow {}^4A_2$ transition is spin forbidden and becomes allowed through spin–orbit coupling to spin quartet states, mainly the $^4T_2$ state, which is energetically close. The transition moment is approximately

$$P_{eff} = \left\langle {}^4A_2 \middle| \mu_E \middle| {}^4T_2 \right\rangle \left\langle {}^4T_2 \middle| H_{so} \middle| {}^2E \right\rangle \Big/ \left[ E({}^2E) - E({}^4T_2) \right] \tag{1}$$

where the dipole operator is $\mu_E$ and the effects of odd-parity distortions are included [6, 10]. The strength of the R line is, therefore, directly related to the strength of the $^4A_2 \leftrightarrow {}^4T_2$ transition. That the R lines in absorption are much stronger for the $\gamma$ centre than for $\alpha$ and $\beta$ confirms that the $^4A_2 \rightarrow {}^4T_2$, $^4T_1$ absorption bands are dominated by absorption from $Cr^{3+}$ ions at centre $\gamma$.

The results of these experiments show that there are three major centres that contribute to the optical spectra of $Cr^{3+}$:$LiNbO_3$. The weak-field $\gamma$ centre is dominant among these three. The decay of the broad-band emission excited in the $^4T_2$ absorption band and detected close to the peak of the $^4T_2$ emission band is dominated by the contribution from the $\gamma$ centre which has a decay time of 10 $\mu$s. A small component of the decay has a lifetime of

about 300 $\mu$s, the decay time associated with the strong-field centres, $\alpha$ and $\beta$ [11]. From the amplitudes of each component in the decay curve, the combined contribution of centres $\alpha$ and $\beta$ to the broad-band intensity is estimated at less than 5%.

### *3.2. Site selective laser excitation spectroscopy*

Site selective excitation and fluorescence line narrowing are useful tools with which to probe multisite systems and inhomogeneously broadened lines. Exciting the $R_2$ component of either centre $\alpha$ or $\beta$ with a narrow-band laser gives rise to luminescence only from the $R_1$ component of the excited centre [9] showing that the $Cr^{3+}$ ions at centres $\alpha$ and $\beta$ do not form an exchange-coupled pair as was suggested by Weiyi *et al* [8]. A sequence of FLN spectra is shown in figure 4. When excited in the low-energy wing of the $^4A_2 \rightarrow {}^4T_2$ absorption (e.g. near $\lambda = 715$ nm) the same three-line pattern is observed as for excitation at higher energies in the same band. At these wavelengths no site selection occurs because the excitation band is vibronically broadened and all centres are equally excited. For excitation wavelengths between 723.5 nm and 725.5 nm there are four lines, three of which are independent of excitation wavelength. The fourth line, which shifts linearly with the laser energy, is due to the close proximity of the $^4T_2$ and $^2E$ levels. At 723.5 nm all of the ions at centres $\alpha$ and $\gamma$ are excited in the $^4T_2$ band as well as a fraction of the $\beta$ centres, giving the same three lines as observed when exciting at 715 nm. In addition, a fraction of the $\beta$ centres are excited in their $R_2$ line, thereby enhancing part of the corresponding $R_1$ line. The same effect is seen for excitation wavelengths around 728 nm: some ions at $\alpha$ centres are excited selectively via their $R_2$ line and non-selectively in their $^4T_2$ band. These experiments show clearly, once again, that the most prominent features of the optical spectra are due to three independent centres. The close proximity of the R lines to each other and to their respective $^4T_2$ bands show that the $^4T_2$ and $^2E$ states are energetically close for all three centres. The crystal field is thus in the intermediate regime though it will be referred to as being strong or weak depending on the lower of the two states as described in the introduction.

There are also two additional, weak, non-resonant features that shift linearly with the laser excitation energy. These are offset from the laser excitation energy by 150 $cm^{-1}$ and 240 $cm^{-1}$, corresponding to Raman spectra reported previously [30]. Whilst these features are not relevant to the present study it is important to know their origin in order to unravel the complicated spectra shown in figure 4.

### *3.3. Measurement of ground state splittings*

The $^4A_2$ ground state is split by non-octahedral components of the crystal field. A trigonal distortion partially lifts the spin degeneracy to give a doublet ground term, $^4A_2(\bar{E})$ and $^4A_2(2\bar{A})$, split by $|2D|$, the so-called zero-field splitting. The $D$ parameter can be measured using electron spin resonance (ESR) and Burns *et al* [5] were the first to do this in $Cr:LiNbO_3$, reporting a single value of $|2D| \simeq 0.90$ $cm^{-1}$. Subsequently, Rexford *et al* [12] reported more sensitive ESR studies, identifying three separate centres, one characterized by $|2D| = 0.822$ $cm^{-1}$, which was identified with the spectrum reported by Burns *et al* [5] on the basis of identical $g$ values. They also reported another spectrum with $|2D| = 0.42$ $cm^{-1}$ and a feature too weak for analysis.

No studies of $Cr : LiNbO_3$ have linked specific ESR spectra to corresponding features in the optical spectra. Optically detected magnetic resonance (ODMR) is a technique which joins the two spectroscopies. Ground and excited state populations perturbed by the

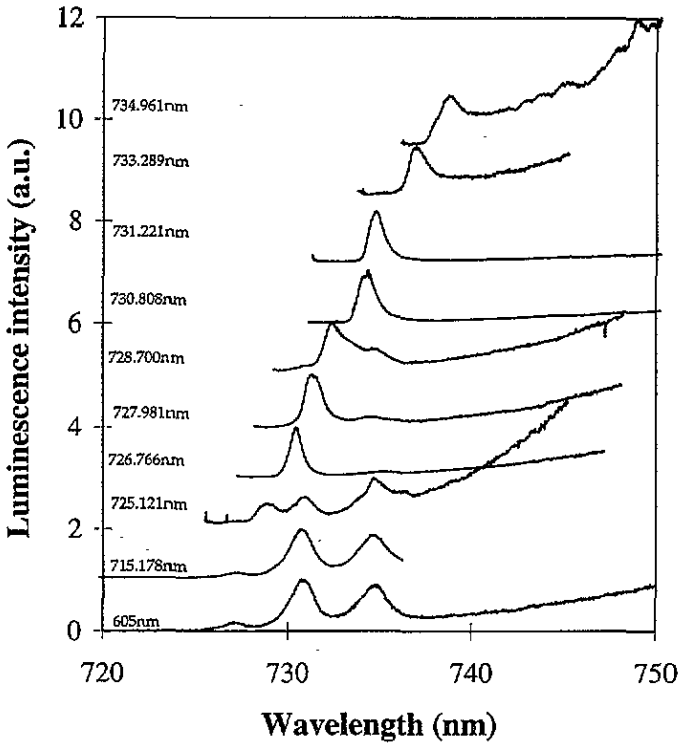


**Figure 4.** Non-resonant FLN spectra of $Cr^{3+}$:$LiNbO_3$ excited in the R line region by a Ti:sapphire laser. The selectively excited fluorescence widths are slit width limited.

application of a resonant microwave field will cause changes in the intensity of the optical spectrum. High-resolution FLN is analogous to ODMR in zero magnetic field. Under these circumstances, the ground state splitting observed can only correspond to the optical centre being excited, making it possible to relate the optical transition to the corresponding ESR spectrum.

The ground state splitting of centre $\alpha$ was measured by high-resolution FLN to be $|2D| = 0.84 \pm 0.02$ cm$^{-1}$ (figure 5(a)). Within experimental error, this corresponds to the zero-field splitting $|2D| = 0.822$ cm$^{-1}$, measured by ESR spectroscopy [5, 12]. The ground state splitting of the R($\beta$) lines is found to be only slightly smaller than that of the R($\alpha$) lines, being given by $|2D| = 0.72 \pm 0.02$ cm$^{-1}$. No such value has been reported in the ESR studies of various authors [5, 12–15]. The close similarity in the R line positions and splittings and of the measured value of $|2D|$ strongly suggest that centres $\beta$ and $\alpha$ are related to the same crystallographic site perturbed in different ways by the disordered nature of the congruently grown $Cr^{3+}$ : $LiNbO_3$ crystal. Note that the slightly greater width of the R($\beta$) lines in figure 3(b) suggests that the optical inhomogeneous broadening is larger for centre $\beta$ than for centre $\alpha$. The associated ESR lines may then be expected to be similarly broadened, making them difficult to distinguish from the $\alpha$ centre lines with which they will almost overlap.

The measured ground state splittings at centres $\alpha$ and $\beta$ are further evidence that these centres do not involve exchange-coupled pairs of $Cr^{3+}$ as has been suggested [8, 13]. In the presence of exchange coupling the Hamiltonian for the two-ion system is classified

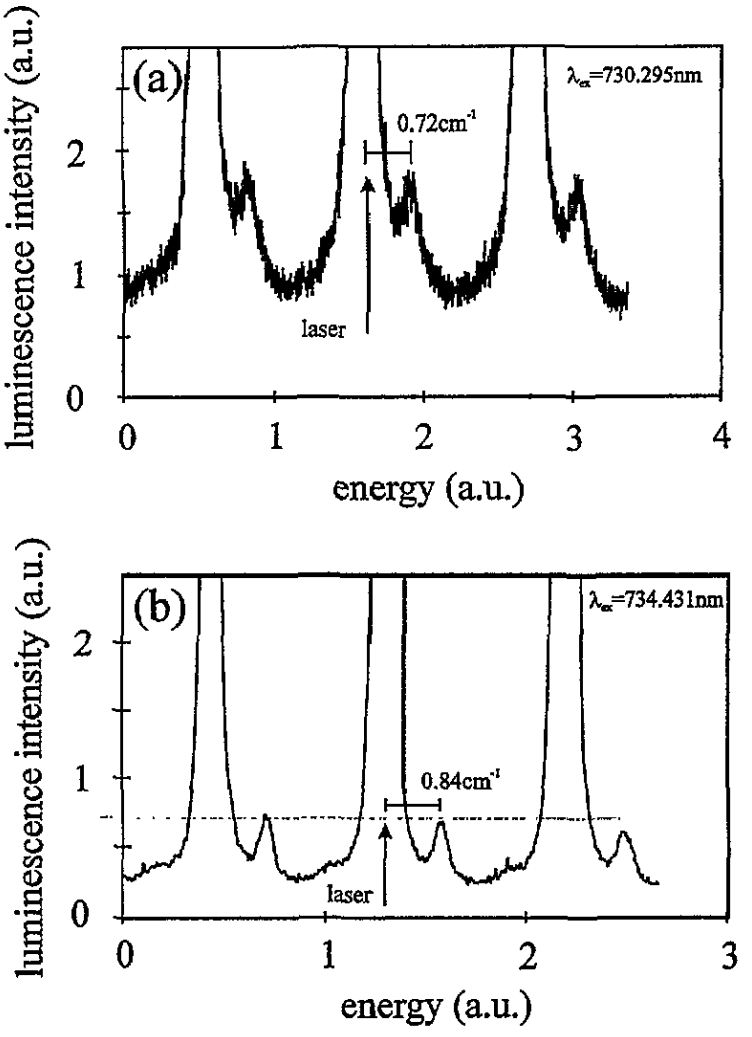


**Figure 5.** FLN spectra showing the ground state splitting of $Cr^{3+}$ ions in (a) the $\beta$ centre and (b) the $\alpha$ centre, measured at 15 K.

according to the total spin $S = S_1 + S_2$. For spin 3/2 ions $S$ can be 0, 1, 2 or 3 and four transitions are commonly observed [17], split approximately by the Landé interval rule [10, 18]. Moreover, for $Cr^{3+}$ concentrations greater than 0.2 at.%, the measured value of $|2D|$ for Cr–Cr pairs is 0.328 $cm^{-1}$ [19], quite different from that of isolated ions. No evidence of R lines characterized by such values of total spin and ground state splitting has been found in the present study.

All previous ESR studies of $Cr:LiNbO_3$ have reported the same centre to be dominant, that with a ground state splitting of $|2D| \approx 0.8$ $cm^{-1}$. It is therefore logical to expect that this spectrum corresponds to the dominant optical centre $\gamma$. The ground state splitting has not been measured optically since the R($\gamma$) lines only fluoresce at high temperatures where the homogeneous linewidth dwarfs the ground state splitting, rendering the FLN technique inoperable. However, Zhao *et al* [20] have calculated the ground state splitting using the method of Macfarlane [21, 22]. This calculation requires a knowledge of $B$, $C$, 10 Dq, the

R line and $^4T_1$ splittings and the spin–orbit coupling parameter. The former four parameters have been discussed and quantified in subsection 3.1 and the $^4T_1$ splitting has been measured from polarized absorption spectra to be 700 $cm^{-1}$ [7]. The spin–orbit coupling parameter is taken to be 210 $cm^{-1}$, a value that has been shown to be correct for other intermediate crystal field hosts [23, 24] and which is consistent with typical values reported for $g_{\|}$ for all centres measured by ESR [25]. Zhao *et al* [20] obtained a value of $2D = 0.748$ $cm^{-1}$ but using the above parameters $2D$ is calculated to be $-0.845$ $cm^{-1}$, in good agreement with the magnitude of 0.822 $cm^{-1}$ measured by ESR [12]. The same centre is therefore shown to dominate both the optical and ESR spectra.

The $^4A_2$ and $^2E$ splittings have been shown to be very similar for all three optically detected centres and so it is concluded that the $\alpha$, $\beta$ and $\gamma$ centres all contribute to the dominant feature in the ESR spectrum. This lends further weight to the argument that the slightly perturbed $\beta$ ESR spectrum is hidden in the wings of the much stronger combined contributions of the $\alpha$ and $\gamma$ centres.

### *3.4. Spectroscopy of Cr:$LiNbO_3$ codoped with magnesium*

Incorporation of $Mg^{2+}$ ions into $LiNbO_3$ has significant influence on the optical properties of the material, including the spectroscopy of $Cr^{3+}$ impurity ions. As figure 2 shows, the absorption spectrum of Cr, Mg:$LiNbO_3$ measured at 77 K has clear differences from that of Cr:$LiNbO_3$, mainly due to the broad absorption bands at 550 nm and 750 nm. These bands are broader than their counterparts in the $Cr^{3+}$ : $LiNbO_3$ spectra; they are assigned to the $^4A_2 \rightarrow {}^4T_2$ and $^4A_2 \rightarrow {}^4T_1$ transitions of a centre that will be referred to as $\delta$. Their energies place the centre firmly in the weak-field regime.

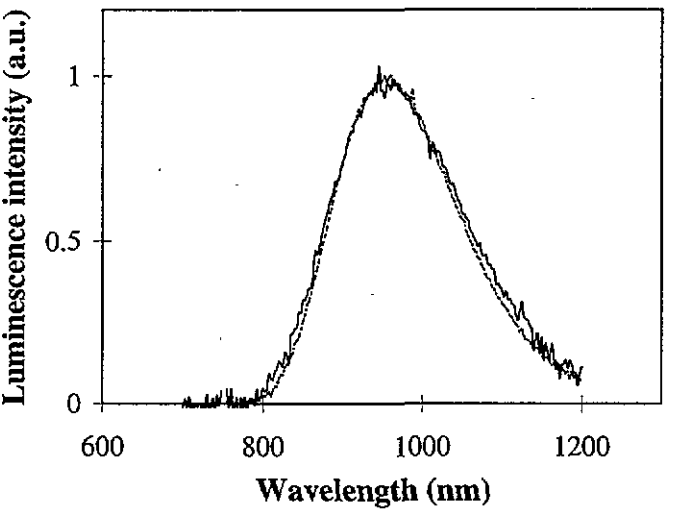


**Figure 6.** Normalized $^4T_2 \rightarrow {}^4A_2$ luminescence spectra in double-doped $Cr^{3+}$, $Mg^{2+}$ : $LiNbO_3$ (dashed line), compared with that of $Cr^{3+}$:$LiNbO_3$. Excitation is at 760 nm in both cases.

The luminescence spectrum of Mg, Cr:$LiNbO_3$ is dominated by a broad $^4T_2 \rightarrow {}^4A_2$ emission band (figure 6). When excited at 760 nm in the $^4A_2 \rightarrow {}^4T_2$ band, where the overlap with the absorption band of the $\gamma$ centre is small, the luminescence spectrum is red shifted by 50 nm compared to the spectrum in figure 3, confirming the $\delta$ centre to have a weaker crystal field than the $\gamma$ centre. The peak of the luminescence band does not depend

significantly on the excitation wavelength except where there are contributions from both centres, suggesting that there is minimal inhomogeneous broadening of the $^4A_2 \rightarrow {}^4T_2$ band of centre $\delta$.

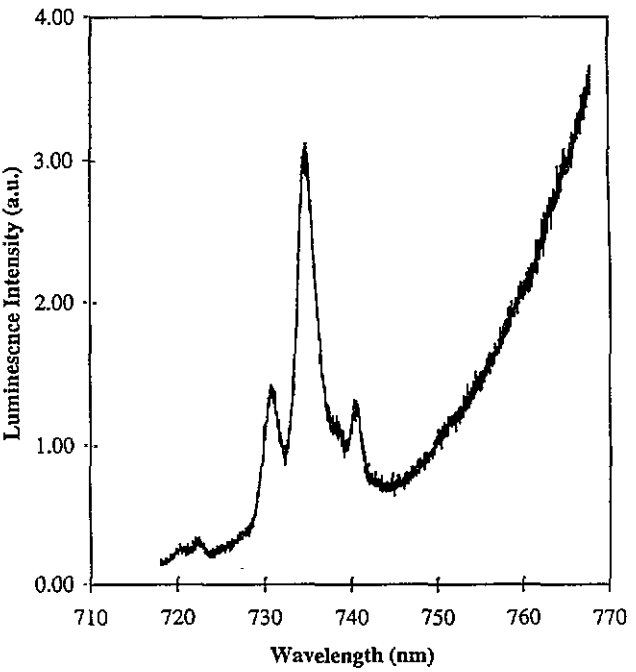


**Figure 7.** The R line luminescence in $Cr^{3+}$, $Mg^{2+}$:$LiNbO_3$, excited at 580 nm. The features at 737.5 nm and 740.5 nm are barely visible in the equivalent $Cr^{3+}$ : $LiNbO_3$ spectrum.

There are also significant differences in the sharp-line luminescence of Mg, Cr:$LiNbO_3$ (figure 7). The lines at 740.5 nm and 737.5 nm have been identified at $^2E \rightarrow {}^4A_2$ transitions related to the $\delta$ centre [16]. If this were the case these R lines would not be observed at low temperature since the zero-phonon line of the $^4A_2 \rightarrow {}^4T_2$ absorption band with a peak at 750 nm should be near 800 nm, some 1000 $cm^{-1}$ lower in energy than the $^2E$ level. Thermal population of the $^2E$ states should be small. In addition, the R lines of a weaker-field centre should be observed at higher photon energy than the R lines of the strong-field centres $\alpha$ and $\beta$. If these additional lines are R lines then they must be due to another centre, centre $\varepsilon$. In consequence, a total of five $Cr^{3+}$ centres are required to interpret the optical spectrum of Mg, Cr:$LiNbO_3$.

Also shown in figure 6 is the luminescence spectrum of the Cr:$LiNbO_3$ sample excited at the same wavelength as the Mg, Cr:$LiNbO_3$ crystal. These spectra have the same lineshape though the intensity is weaker in the case of the Cr:$LiNbO_3$ sample. The R line at 739.1 nm has been observed in Cr:$LiNbO_3$ [26] and in the resonantly excited *FLN* spectra in figure 4 excited at wavelengths exceeding 735 nm. These results suggest that the effect of codoping $LiNbO_3$ with $Mg^{2+}$ and $Cr^{3+}$ is not to create additional centres associated with Cr–Mg complexes but rather to increase substantially the density of those centres already present in low concentrations in Cr:$LiNbO_3$.

### *3.5. Charge compensation and site occupation of $Cr^{3+}$ in $LiNbO_3$*

It has been shown above that there are contributions from five centres to the optical spectra of $Cr^{3+}$ in $LiNbO_3$. Centres $\alpha$, $\beta$ and $\gamma$ all contribute to the dominant signal recorded in the ESR spectra. As the $\gamma$ centre dominates the optical spectra it is reasonable to assume that the $\alpha$ and $\beta$ centres are perturbed $\gamma$ centres. Although the $\delta$ and $\varepsilon$ centres increase in intensity with the addition of $Mg^{2+}$ ions to the crystal they are also present in magnesium-free material. The physical nature of these five centres is now discussed.

Previous studies have taken both theoretical and experimental approaches. The nature of the dominant $\gamma$ centre was first discussed by Glass [7]. Partially on the basis of a point ion calculation Glass proposed that $Cr^{3+}$ substitutes preferentially at the $Nb^{5+}$ site, and that the necessary charge compensation was by oxygen vacancies. Michel-Calendini *et al* [27] calculated the energies of $Cr^{3+}$ in the $Li^+$ and $Nb^{5+}$ sites using a molecular orbital model. They determined that when $Cr^{3+}$ occupies the central position in the $Li^+$ octahedron then that site is slightly favoured over the equivalent position in the $Nb^{5+}$ octahedron. However, Chang *et al* [28] stressed the importance of using the more precise $C_3$ site symmetry in their calculations rather than the simplifying assumption of $C_{3v}$ symmetry used by others. They derived spin-Hamiltonian terms using superpositions of single ligand contributions and diagonalized the crystal field matrix to obtain the energy levels of $Cr^{3+}$ in the $Li^+$ and $Nb^{5+}$ sites. Their results appeared to support $Cr^{3+}$ substitution at both sites. However, they claimed that only $Cr^{3+}$ occupancy of the $Nb^{5+}$ site accounted for the main ESR spectrum. In earlier studies the same claim had been made for the $Li^+$ site [29, 30]. A cluster model analysis of the properties of the $Cr^{3+}$–$Cr^{3+}$ pair complex proposed by Weiyi *et al* [8] supported the dimeric charge compensation mechanism [31], now discredited as discussed above and in [9].

Theoretical approaches that rely to a great extent on optimizing free parameters to fit experimentally determined energies fail to determine the site occupation of $Cr^{3+}$ in the various sites in $LiNbO_3$. This is unsurprising given that the R lines are rather insensitive to changes in the crystal field, that the $Nb^{5+}$ and $Li^+$ ions have almost equal orbital radii, that the charge misfit is identical for $Cr^{3+}$ entering either of the substitutional sites and that the sizes of the octahedral sites are similar. When the defect models and their energy level structure are based on incorrect interpretation of spectroscopic data [32] with good agreement between model and experiments still being claimed [28, 29], the theoretical approach may be inappropriate. In reality the differences in the energy level structure of $Cr^{3+}$ ions in the different locations in $LiNbO_3$ are so slight that the theoretical models cannot reliably distinguish between the particular spectral features of particular defect sites. In consequence, the best approach to the assignment of the site occupation of $Cr^{3+}$ in $LiNbO_3$ is on the basis of the experimental results.

A purely experimental approach was taken by Rexford *et al* [12] who suggested that the three ESR spectra they observed corresponded to $Cr^{3+}$ ions in the $Nb^{5+}$ and $Li^+$ sites and the empty octahedron. Grachev *et al* [13] argued on the basis of ESR and ENDOR studies that the $Cr^{3+}$ ions entered both the $Li^+$ and $Nb^{5+}$ sites, charge compensation for $Cr^{3+}$ at concentrations of less than 0.2% being by a pairing process involving $Cr^{3+}$ ions and other neighbouring impurity cations (e.g. $Al^{3+}$ or $Fe^{3+}$). The incorporation of $Al^{3+}$ and $Fe^{3+}$ ions into the crystal is accidental and different samples grown in different laboratories would not have the same concentrations of accidental impurities. All published optical spectra of Cr : $LiNbO_3$ are very similar so the different centres are unlikely to be due to this charge compensation mechanism. Nicholls *et al* [9] agreed that $Cr^{3+}$ would occupy both the $Li^+$ and $Nb^{5+}$ sites, arguing from the crystal-field calculations of Glass [7] that the R($\alpha$)lines

are due to $Cr^{3+}$(Li) sites and the R($\beta$) lines to $Cr^{3+}$(Nb) sites. All of these models have been proved to be wrong by the present study, which shows that the main $Cr^{3+}$ centres in $LiNbO_3$ are associated with the same site.

Rutherford backscattering experiments in Nd-doped $LiNbO_3$ [33] have identified three inequivalent $Nd^{3+}$ sites which are due to there being three stable positions for $Nd^{3+}$ within the lithium octahedron, all different from the natural position of lithium. The $Nd^{3+}$ ions then experience three different trigonal fields resulting in different splittings but the same barycentre for the transitions. The effect has been attributed to different methods of charge compensation. Such a mechanism does not seem likely for Cr:$LiNbO_3$. The $\alpha$, $\beta$ and $\gamma$ centres have very similar ground and excited state splittings, suggesting that the trigonal field is approximately the same in each case. If the strong field R lines are associated with separate charge compensators their effect would rather be to change the Racah $B$ parameter or apply an $A_{1g}$ totally symmetric distortion to the octahedron.

The most comprehensive study of the ground state ESR spectra of $Cr^{3+}$:$LiNbO_3$ has been performed by Corradi *et al* [14]. The most intense ESR signal, corresponding to centre $\gamma$, was assigned from ESR and ENDOR studies to the $Cr^{3+}$(Li) site. The ability of the ENDOR technique to determine the nearest-neighbour ions of the impurity ion under investigation makes this study very reliable.

A natural mechanism for $\alpha$, $\beta$ and $\gamma$ centres to be associated with the $Li^+$ site in $LiNbO_3$ is provided by the compositional disorder of the crystal, at least in crystals grown from the congruently melting composition. $Nb^{5+}$ ions occupy 5.9% of $Li^+$ sites and a slightly smaller fraction (4.7%) of $Nb^{5+}$ vacancies are required for charge compensation. These intrinsic imperfections in $LiNbO_3$ occur in far greater concentrations than the most common impurities [34]. Changes in the charge distribution caused by the defects influence the energy levels of the $Cr^{3+}$ ion. It is reasonable to expect that defects in the second-nearest-neighbour shell (a cation shell) will have the strongest effect. The $Li^+$ site, shown in figure 1, is surrounded by an approximate octahedron of $Nb^{5+}$ sites and a slightly larger, rotated octahedron of $Li^+$ sites. With the $Nb^{5+}$ site along the $c$ axis at approximately the same distance this gives seven second-nearest-neighbour $Nb^{5+}$ ions and six $Li^+$ ions. In consequence, it is expected that some $Cr^{3+}$ ions have a neighbouring $Nb^{5+}$ vacancy or an $Nb^{5+}$ antisite as occasional alternatives to the perfect lattice configuration. Assuming a Poissonian distribution of defects, 49% of $Cr^{3+}$ ions in $Li^+$ sites should occupy sites with no second-nearest-neighbour defects, 17% should have one Nb vacancy and 18% one Nb antisite. The almost equal intensities of $R_1(\alpha)$ and $R_1(\beta)$ lines suggest that the numbers of $Cr^{3+}$ ions in the $\alpha$ and $\beta$ centres are approximately equal. The actual intensities of the $R_1(\alpha)$ and $R_1(\beta)$ lines are weaker than would be expected from a purely statistical occupation hypothesis but the simple model does predict three dominant centres, one of which is much more common than the other two almost equally populous perturbed sites. The proportion of $\alpha$ and $\beta$ centres is higher than would appear from a simple inspection of the fluorescence spectra because these centres also decay via the broad band (see subsection 3.1), thus reducing the intensities of their R lines. Furthermore, there is evidence that defects are not entirely free and tend to form clusters, thus reducing the number of isolated defects [34]. Hence, it would be expected that the proportion of $Cr^{3+}$ ions occupying defect centres would be reduced. It is concluded therefore that the $\gamma$ centre is the undistorted $Li^+$ site and the $\alpha$ and $\beta$ centres are $\gamma$ centres distorted by the presence of either a $Nb^{5+}$ vacancy or antisite.

The addition of $Mg^{2+}$ causes increased occupation of the $\delta$ and $\varepsilon$ optical centres. In a comparative study of Cr:$LiNbO_3$, Cr, Mg:$LiNbO_3$ and ruby, Thiemann *et al* [15] reported an additional $Cr^{3+}$ centre with isotropic ESR spectrum ($D < 0.01$ cm$^{-1}$) to be present in

$LiNbO_3$ co-doped with $Cr^{3+}$ and $Mg^{2+}$ and that this was responsible for the additional absorption bands. ENDOR results had already proved that $Cr^{3+}$ could substitute in a $Nb^{5+}$ site [14]. The authors believed that the ENDOR parameters (hyperfine splitting, quadrupole splitting, axial field splitting) were so different from those of the centre with $|2D| = 0.822$ $cm^{-1}$ that the two centres relate to different sites. Thiemann *et al* [15] inferred that in Cr:$LiNbO_3$ the $Cr^{3+}$ ion must substitute for $Li^+$ and that the addition of $Mg^{2+}$ forces $Cr^{3+}$ into the $Nb^{5+}$ site. This suggestion does not conflict with the proposals made here. By analogy with the $Li^+$ sites, it is thought that the weak-field $\delta$ centre is the undistorted $Nb^{5+}$ site while the strong-field $\varepsilon$ centre is a $Nb^{5+}$ site perturbed by a nearby vacancy or antisite. A summary of parameters relating to all five centres is given in table 2.

**Table 2.** A summary of the site occupation and energy levels of the $Cr^{3+}$ centres in $LiNbO_3$.

| Centre | $^2E$ energy ($cm^{-1}$) | $^2E$ splitting ($cm^{-1}$) | Broad-band fluorescence peak ($cm^{-1}$) | Site occupation |
|---|---|---|---|---|
| $\alpha$ | 13640 | 95 | n/a | Li (distorted) |
| $\beta$ | 13720 | 64 | n/a | Li (distorted) |
| $\gamma$ | 13790 | 38 | 11100 | Li |
| $\delta$ | not observed | not observed | 10500 | Nb |
| $\varepsilon$ | 13532 | 55 | n/a | Nb (distorted) |

## 4. Conclusions

The history of Cr:$LiNbO_3$ spectroscopy has been shrouded in confusion. Until this study no authors had recognized the fact that three centres are required to account for the R lines that they had observed [5, 7–9, 16, 26, 28, 29, 32]. There were suggestions that R lines are hot-phonon side bands and exchange-coupled pairs [8]. In other reports R lines have been paired with partners having wildly different absorption and fluorescence characteristics [32]. The further study of Mg, Cr:$LiNbO_3$ has added to the confusion. It has been supposed that the $Mg^{2+}$ ions create a new optical centre and that this centre emits through R line and broad-band fluorescence despite the $^2E$ state being about 1000 $cm^{-1}$ above the $^4T_2$ state [16].

The present study has resolved the difficulties in interpretation of the spectra. The results of many optical and ESR studies have been integrated through the optical measurement of the ground state splittings of the main centres in Cr:$LiNbO_3$. It has been shown that the principal centres in Cr:$LiNbO_3$ are all the result of $Cr^{3+}$ substitution at $Li^+$ sites. The main centre that dominates both ESR and optical spectra is the undistorted $Li^+$ site but R line fluorescence derives from $Li^+$ sites that are perturbed by nearby Nb vacancies or antisites. *The addition of $Mg^{2+}$ to the lattice causes $Nb^{5+}$ sites to be more preferentially occupied* and a weak and a strong field centre relating to $Cr^{3+}$ occupation of the $Nb^{5+}$ site become more predominant in the optical spectra. The $Nb^{5+}$ sites are weaker field sites than the $Li^+$ sites and so it must be assumed that long-range charge compensation is more easily achieved for the $Li^+$ sites, causing them to be preferred. The addition of $Mg^{2+}$ to the lattice alters the fine balance in favour of the $Nb^{5+}$ sites. It is likely that there are other much weaker features in the optical and ESR spectra of Cr : $LiNbO_3$ that relate to $Li^+$ and $Nb^{5+}$ sites perturbed by other combinations of antisites and vacancies. However, the five main optical centres have now been accounted for.

## Acknowledgments

KH thanks the Nuffield Foundation for partial support of his work and PIM thanks DRA Malvern and EPSRC for support of his study through a CASE studentship. The samples used in this study were grown at the Universidad Autonoma de Madrid.

## References

[1] Abrahams S C, Reddy J M and Bernstein J L 1966 *J. Phys. Chem. Solids* **27** 997
[2] Weiss R S and Graylord T K 1985 *Appl. Phys.* A **37** 191
[3] Sviridov D T and Sviridova R K 1971 *Sov. Phys.–Solid State* **15** 715
[4] Abrahams S C and Marsh P 1986 *Acta Crystallogr.* B **42** 61
[5] Burns G, O'Kane D F and Title R S 1966 *Phys. Lett.* **23** 56; 1968 *Phys. Rev.* **167** 314
[6] Sugano S, Tanabe Y and Kamimura H 1970 *Multiplets of Transition Metal Ions in Crystals* (New York: Academic)
[7] Glass A M 1969 *J. Chem. Phys.* **50** 1501
[8] Weiyi J, Liu H, Knutson R and Yen W M 1990 *Phys. Rev.* B **41** 10906
[9] Nicholls J F H, Han T P J, Henderson B and Jaqué F 1993 *Chem. Phys. Lett.* **202** 560
[10] Henderson B and Imbusch G F 1990 *Optical Spectroscopy of Inorganic Solids* (Oxford: Oxford University Press)
[11] Macfarlane P I, Holliday K and Henderson B *Phys. Rev. Lett.* submitted
[12] Rexford D G, Kim Y M and Story H S 1970 *J. Chem. Phys.* **52** 860
[13] Grachev V G, Malovichko G I and Troitskii V V 1987 *Sov. Phys.–Solid State* **29** 349
[14] Corradi G, Sothe H, Spaeth J-M and Polgar K 1991 *J. Phys.: Condens. Matter* **3** 1901
[15] Thiemann O, Corradi G and Reyher H J 1992 *Ferroelectrics* **125** 283
[16] Camarillo E, Tocho J, Vergara I, Dieguez E, Garcia-Solé F J and Jaqué F 1992 *Phys. Rev.* B **45** 4600
[17] Abragam A and Bleaney B 1986 *Electron Paramagnetic Resonance of Transition Ions* (New York: Dover)
[18] Geschwind S 1972 *Electron Paramagnetic Resonance* ed S Geschwind (New York: Academic)
[19] Siu G G and Zhao M G 1991 *Phys. Rev.* B **43** 13575
[20] Zhao M G, Yan Q L and Siu G G 1995 *Phys. Status Solidi* b **187** K13
[21] Macfarlane R M 1967 *J. Chem. Phys.* **47** 2066
[22] [20] and [21] state the same formula in slightly different form. The present work uses [21]. Using the formula quoted in [20] gives a value of $2D = -0.823\ \mathrm{cm}^{-1}$.
[23] Struve B and Huber G 1985 *Appl. Phys.* B **36** 195
[24] Grinberg M, Macfarlane P I, Henderson B and Holliday K 1995 *Phys. Rev.* B **52** 3917
[25] Yeom T H, Chang Y M, Rudowicz C and Choh S H 1993 *Solid State Commun.* **87** 245
[26] Nicholls J F H 1995 *PhD Thesis* University of Strathclyde
[27] Michel-Calendini F M, Bellafrouh K and Daul C 1992 *Ferroelectrics* **124** 271
[28] Chang Y M, Yeom T H, Yeung Y Y and Rudowicz C 1993 *J. Phys.: Condens. Matter* **5** 6221
[29] Chang Y M, Wen J K and Wang H F 1992 *Chin. Phys. Lett.* **9** 427
[30] Martin A, Lopez F J and Aguillo-Lopez F 1992 *J. Phys.: Condens. Matter* **4** 847
[31] Qiu Y 1993 *Phys. Rev.* B **48** 4868
[32] Camarillo E, Garcia-Sole J, Cussó F, Aguillo-Lopez F, Sanz-Garcia J A, Han T P J, Jaqué F and Henderson B 1991 *Chem. Phys. Lett.* **185** 505
[33] Garcia-Solé F J, Petit T, Jaffrezic H and Boulon G P 1993 *Europhys. Lett.* **24** 719
[34] Donnerburg H, Tomlinson S M, Catlow C R A and Schirmer O F 1989 *Phys. Rev.* B **40** 11909